Scientific Reports

https://doi.org/10.1038/s41598-026-38169-4

Article in Press

New perspectives on the ozonated high-oleic sunflower oil physico-chemical behaviour

Received: 1 October 2025

Accepted: 29 January 2026

Published online: 02 February 2026

Cite this article as: Petrovici A., Paraschiv V., Nicolescu A. *et al.* New perspectives on the ozonated high-oleic sunflower oil physico-chemical behaviour. *Sci Rep* (2026). https://doi.org/10.1038/s41598-026-38169-4

Anca-Roxana Petrovici, Vasile Paraschiv, Alina Nicolescu, Mirela-Fernanda Zaltariov, Maria Bercea, Natalia Simionescu & Mariana Pinteala

New Perspectives on the Ozonated High-Oleic Sunflower Oil Physico-Chemical Behaviour

Anca-Roxana Petrovici[a]*, Vasile Paraschiv[b], Alina Nicolescu[c], Mirela-Fernanda Zaltariov[d], Maria Bercea[e], Natalia Simionescu[a], Mariana Pinteala[a]

[a] Centre of Advanced Research in Bionanoconjugates and Biopolymers Department, "Petru Poni" Institute of Macromolecular Chemistry, 41A Grigore Ghica Voda Alley, 700487 Iasi, Romania;

[b] SC OVVA IASI SRL, 707025 Baltati-Iasi, Romania; vasileparaschivro@gmail.com;

[c] NMR Laboratory, "Petru Poni" Institute of Macromolecular Chemistry, Aleea Grigore Ghica Voda, 41 A, 700487, Iasi, Romania.

[d] Department of Inorganic Polymers, "Petru Poni" Institute of Macromolecular Chemistry, Aleea Grigore Ghica Voda, 41 A, 700487, Iasi, Romania.

[e] Polyaddition and Photochemistry Department, "Petru Poni" Institute of Macromolecular Chemistry, Aleea Grigore Ghica Voda, 41 A, 700487, Iasi, Romania.

[*] Corresponding author: Anca-Roxana Petrovici, petrovici.anca@icmpp.ro

Funding: This work was supported by a grant of the Ministry of Research, Innovation and Digitization, CNCS/CCCDI - UEFISCDI, project number PN-IV-P8-8.1-PRE-HE-ORG-2023-0048, within PNCDI IV.

Abstract:

Despite high-oleic sunflower oil (SFO) having strong antioxidant properties, there are very few studies regarding its physico-chemical characterization. In this study, SFO obtained through cold pressing, without prior chemical treatment, was subjected to an ozonation process. Simultaneously, a water-SFO emulsion (1:9 ratio) was prepared and ozonated in the same conditions. Both ozonated samples underwent physico-chemical evaluation (acid and peroxide values (AV, PV), rheological behaviour), structural analyses, and antioxidant properties evaluation. Through their AV and PV, the samples demonstrate excellent stability over time, from an AV of 3.073 to 3.723 mg NaOH/g oil and from a PV of 1439.36 to 1645.29 mmol/equiv/g oil over 6 months storage for ozonated SFO. The viscosity and flow activation energy increase with ozonation time and are superior to those of raw oil. The NMR and FTIR analyses reveal a high ozonation degree over time, acting according to Criegee's mechanism, and the water presence accelerates the ozonation process. Both sample types exhibited a strong capacity to neutralize free radicals, a high affinity for binding Fe^{2+} ions, and remarkable efficacy in protecting lipid membranes. The results obtained in our study bring important high novelty contributions in the field of ozonated sunflower oils, make it a promising candidate for future in-vivo testing.

Keywords: high oleic high-oleic sunflower oil, ozonated high-oleic sunflower oil, antioxidant properties, NMR, FTIR, oil rheology.

1. Introduction

In recent years, farmers' interest in growing high-oleic sunflowers has increased. This is because these particular sunflower seeds have a high oleic acid content of over 70 to 90%. These characteristics make it as nutritionally valuable as olive, rapeseed or flaxseed oils, with a high antioxidant potential [1,2].

Sunflower oil (SFO) is one of the most valued seed oils, recognized for its pale colour and balanced fatty acid composition. Its main components are oleic and linoleic acids, but the composition can vary between species, the plants' and seeds' maturation stage, or temperature. More than that, the oleic acid content is greatly influenced by climatic conditions, especially by differences between day and night temperatures [3]. Moreover, it is rich in compounds (besides their characteristic fatty acid profile) that act as antioxidants and can mitigate free radicals, diminishing inflammation or oxidative stress, which helps in the management of different illnesses, like cardiovascular and dermatological issues [4,5].

A major drawback of vegetable oils, including SFO, is that their component fatty acids are susceptible to autooxidation, a process that involves a chain reaction mechanism in the presence of molecular oxygen *via* free radicals. The free radicals are formed by the adduction of a hydrogen atom that quickly reacts with molecular oxygen to produce a peroxyl radical, able to propagate the reaction with a parallel accumulation of fatty acid hydroperoxides, which are unstable and have the tendency to break down into carbonylic fragments or react with other oxygenated species [6,7]. As a result, ketones, epoxides, acids, or ethers are generated that are responsible for the characteristic rancid odour of autooxidised vegetable oils [5,8,9]. Nevertheless, SFO contains non-polar antioxidants, including α-tocopherol, which play a role in the oxidative stability of the fatty acid profile [10]. Furthermore, some research groups are closely involved in research on increasing the stability of SFO over time by supplementing it with either synthetic [11] or natural [12] antioxidant compounds.

Moreover, vegetable oils have been shown to readily react with ozone (O_3), leading to a rapid increase in peroxide values. Ozone, an allotropic form of oxygen, is widely applied across scientific, medical, and industrial fields due to its strong oxidizing properties. It reacts much faster than oxygen with electron donors, making it highly effective in various applications. Ozone is recognized for its potential therapeutic benefits in treating a range of illnesses, but its effects are heavily influenced by the dosage and method of administration, requiring carefully designed therapeutic plans [6,13]. The ozone amount that oils are capable of integrating depends on the fatty acids' unsaturation degree. However, the chemical characterization of ozonated vegetable oils is difficult due to the large variety of oxygenated species. Despite this complexity, grape seeds, sunflower, olive or soybean ozonated oils, have been efficaciously applied as complementary agents with anti-inflammatory, antibacterial, and wound-healing properties [13,14]. These oil types have also shown antiallergic potential and are frequently used in dermatology and cosmetic therapies [15].

One important characteristic of the ozonated vegetal oils is their ability to stabilize ozone in a proper chemical structure that allows its biological activity. Among the therapeutic effects of these ozonated oils, the literature mentions a significant acceleration of the first phase of skin wound healing for sunflower, olive, sesame and linseed ozonated oils' treatment [15,16] or the embryos and cells protection due to the antimicrobial and antioxidant activities of the ozonated SFO [17]. Other scientifically proven benefits of ozonated SFO are

amelioration of dyslipidemia, hepatic inflammation, oxidative stress and protection against toxicity caused by carboxymethyl lysine [18].

To our knowledge, there are very few publications on the high-oleic SFO characterization, and furthermore, there are no published studies on ozonated SFO that include rheological characterization, NMR spectroscopy, or antioxidant activity evaluated through comparative studies. Furthermore, no studies have employed a comprehensive set of antioxidant evaluation methods such as ABTS, DPPH, hydroxyl and superoxide anion radicals' scavenging assays, FRAP, ferrous ion chelating activity, or lipid peroxidation inhibitory assay.

In this order, our study brings important high novelty contributions in the field of ozonated high-oleic SFOs, by aiming to produce a natural, organic SFO without any chemical modifications, which, after ozonation, could become a product with significant therapeutic potential. To achieve these objectives, the high-oleic sunflower plants were cultivated under organic conditions, and the oil was cold-pressed and stored at low temperatures in hermetically sealed containers. A portion of the oil was ozonated directly, while another portion was mixed with water and ozonated under identical conditions. The resulting products were thoroughly characterized in terms of their physico-chemical properties, including antioxidant properties through eight different methods with the aim of highlighting a complex characterization. The findings from this research indicate that the ozonated high-oleic samples exhibit a high therapeutic potential and curative properties, making them promising candidates for future *in-vivo* testing.

2. Materials and methods

2.1. Vegetal materials

PIONEER P244 untreated high-oleic sunflower seeds were organically cultivated in Vetrisoaia, Vaslui region, Romania. They were sown in late April and harvested in early September (2023). The seeds were stored in fibre bags under controlled humidity conditions and at a temperature below 18 °C until December 2023, when they were pressed.

2.2. SFO extraction

The SFO was extracted from seeds using a pressing platform in which the oil was immediately filtered (using filter cards no. 1, 200/200mm) and bottled. COTER S205/60 oil extraction platform was purchased from Coter Franco, Italy, with a pressing capacity about 20 kg seeds/hour. The oil temperature at the outlet of the pressing head did not exceed 40-45 °C. The seeds were pressed without heat treatment. The oil extraction yield was 35%. After extraction, the oil was stored at 8 °C in hermetically sealed glass containers.

2.3. Ozonation procedure

The high-oleic oil ozonation was carried out in 400 mL SFO or water-SFO emulsion (1:9 ratio), using a glass container with 5 cm diameter and 40 cm height, in which the ozone was bubbled in a concentration of 4.5 g ozone/hour over 12 hours. The temperature during bubbling was maintained between 18-20 °C using a cooling water bath. The ozone generator used was OxyCare Black 5, produced by SC AZURE LAB SRL (Romania) with the capacity to generate 5 g ozone / hour. Only oxygen was used for ozonation, using a DeVilbiss KS 525

oxygen concentrator (DRIVE MEDICAL GMBH & CO. KG, Germany), at a flow rate of 3 L/min.

2.4. Acid value (AV) analysis

The Acid Value (AV) represents the amount of sodium hydroxide required to neutralize all the free acids present in a specific quantity of oil. For this procedure, 0.5 g of each oil sample was weighted, dissolved in 17 mL of ethanol (Sigma-Aldrich, Catalogue no.459844-4X2.5L, ≥99.5%), and titrated with 0.1 M sodium hydroxide (Merk, Catalogue no. 1064980500, p.a. reagent) in the presence of phenolphthalein (Merk, Catalogue no. 1072330025, ACS reagent) until a pale pink colour persisted [14]. Each sample was analysed in triplicate, and the AV was calculated using the equation (1) provided below:

$$AV\ (mg\ NaOH/g\ oil) = M * c * V/w \quad (1)$$

where: M - the NaOH molar mass; c - the NaOH concentration; V - the NaOH volume used; w - the oil sample mass.

2.5. Peroxide value (PV) analysis

The peroxide values (PV) of SFO were analysed using an iodometric assay after 24 hours reaction time. The PV indicates the milliequivalents of active oxygen present in 1,000 g of the substance, representing the amount of peroxide formed. Briefly, 0.25 g of each sample was thoroughly mixed with 15 mL of a solvent mixture composed of glacial acetic acid (Merk, Catalogue no. 1000631000, 100%) and chloroform (Merk, Catalogue no. 8222651000, ≥99%) in a 3:2 (v/v) ratio. Following this, 0.25 mL of saturated potassium iodide (Sigma-Aldrich, Catalogue no.60400-100G-F, ≥99%) solution was added, and the mixture was stored in darkness. After 24 hours, 15 mL of water was added, and the solution was titrated slowly with 0.05 N sodium thiosulphate (Supelco, Catalogue no. 1065120250, anhydrous) in the presence of starch (Sigma-Aldrich, Catalogue no. 33615-250G, p.a.), continuing until the blue colour disappeared. Each sample was analysed in triplicate, the PV was expressed in mmol/equiv/g oil [7] and calculated using the following equation (2):

$$PV\ (mmol/\ equiv/g\ oil) = V * C * 1000/W \quad (2)$$

where: V - mL of sodium thiosulphate volume consumed in the titration; C - sodium thiosulphate concentration; W – oil samples weight in g.

2.6. Rheological measurements

The viscosity measurements were performed with a MCR 302 rheometer (Anton Paar, Graz, Austria), using a plane-plane geometry (the upper plate with the diameter of 25 mm and the gap of 0.5 mm) and Peltier device for a rigorous temperature control. The viscosity was measured over a large temperature range, from 0 °C to 100 °C. The shear viscosity (η) was measured as a function of the shear rate ($\dot{\gamma}$) in stationary continuous shear conditions, from 0.001 s^{-1} to 1000 s^{-1}.

2.7. Nuclear Magnetic Resonance (NMR) analysis

The NMR spectra of all samples included in this study were recorded on a Bruker Avance Neo 400 MHz spectrometer (Bruker Optics, Ettlingen, Germany), equipped with a 5

mm direct detection, four nuclei (H, C, F, Si), z-gradient probe. For the NMR analysis, the samples were prepared by thoroughly mixing 0.5 mL oil with 0.5 mL deuterated chloroform (Deutero GmbH, Germany) and transferred in 5 mm NMR tubes. The chemical shifts are reported in ppm relative to solvent signal ($CDCl_3$ ^{1}H: 7.26 ppm and ^{13}C: 77.01 ppm). The exact signals assignments for newly formed oxygenated derivatives were obtained from the following 1D and 2D experiments: 1D 13C-NMR, 1D carbon edited DEPT135 (Distortionless Enhancement by Polarization Transfer), 2D homonuclear proton-proton correlation experiment H,H-COSY (Correlation Spectroscopy) and 2D heteronuclear proton-carbon direct bond correlation experiment H,C-HSQC (Heteronuclear Single Quantum Coherence).

2.8. Fourier Transform Infrared Spectroscopy (FTIR) analysis

IR spectra were registered at room temperature in Attenuated Total Reflectance (ATR) mode in the 600-4000 cm^{-1} with a resolution of 2 cm^{-1} and accumulation of 32 scans by using a FT-IR spectrometer Vertex 70 (Bruker Optics, Ettlingen, Germany) equipped with ATR module having a ZnSe crystal (PIKE MIRacle Technologies). Before recording, the samples were applied as thin films directly on the surface of the ZnSe crystal. The spectra have been processed with OPUS 6.5 software: water and CO_2 compensation, baseline correction, normalization and 2nd derivative function. The 2nd derivative of the spectra was used to highlight the hidden and overlapped peaks.

2.9. Antioxidant properties

The assessment of antioxidant properties was performed on all SFO samples, which were diluted in ethanol at a concentration of 45 μg/mL, and the results were compared with those obtained for Trolox (Sigma-Aldrich, Catalogue no.238813-5G, ≥97%) (45 μg/mL) and Ascorbic acid (Sigma-Aldrich, Catalogue no.A92902-100G, ≥99%) (AA; 45 μg/mL), as common antioxidant references. All experiments were performed in triplicate. Each test was finished by reading the respective absorbance in 100 μL reaction mix placed in a 96-well plate in triplicate, using a FLUOstar® Omega microplate reader (BMG LABTECH, Ortenberg, Germany).

2.9.1. ABTS radical scavenging assay

The samples' $ABTS^{+}$• scavenging properties were determined as previously described by Petrovici et al. [19], in brief, 1.2 mL of $ABTS^{+}$• reagent (which were obtained by mixing 0.35 mL of 7.4 mM ABTS diammonium salt (Sigma-Aldrich, Catalogue no. A1888-2G, ≥98% HPLC) with 0.35 mL of 2.6 mM potassium persulfate (Sigma-Aldrich, Catalogue no.216224-100G, ≥99%), and kept in the dark at room temperature for 16 h, then diluted 1:50 with 95% ethanol (Sigma-Aldrich, Catalogue no.459844-4X2.5L, ≥99.5%)) was mixed with 0.3 mL of each sample, AA and Trolox as references or ethanol as negative control. The samples were kept for 6 minutes in the dark, then the absorbance was measured at 734 nm. The samples' ABTS• inhibition percentage was calculated using the equation (3):

$$ABTS^{\bullet}\ Inhibition\ \% = (1 - As/Ao) \times 100 \quad (3)$$

where A_S is the sample absorbance and A_0 is the blank absorbance [19].

2.9.2. DPPH radical scavenging assay

The DPPH radical scavenging activity was performed following the procedure published by Petrovici et al. [19], 1000 µL DPPH (Sigma-Aldrich, Catalogue no. D9132-5G, ≥99.5%) (89.7 µM in methanol) was mixed very well with 500 µL of each sample, AA, Trolox or ethanol as negative control, then left in the dark for 2 hours. After the reaction was complete, the absorbance was measured at 517 nm, and the DPPH• inhibition percentage of the samples was calculated using the equation (4):

$$DPPH^{\bullet}\ Inhibition\ \% = (1 - As/Ao) \times 100 \quad (4)$$

where A_S is the sample absorbance and A_0 is the blank absorbance [19].

2.9.3. Hydroxyl Radical ($HO^{\bullet}$) Scavenging Ability

The $HO^{\bullet}$ scavenging ability was determined using the published experimental protocol [20] as follows: 400 µL of each sample, AA, Trolox, H_2O_2 and ethanol as negative control was mixed with 400 µL O-phenanthroline (Acros Organics, Catalogue no. 417120050, ACS reagent) (2.5 mM) and 400 µL PBS (Sigma-Aldrich, Catalogue no. P4417-100TAB), 0.2 M, pH 7.4. After a vigorous mixing, 400 µL of ferrous sulphate heptahydrate (Sigma-Aldrich, Catalogue no. 215422-250, ≥99%) (2.5 mM) and 400 µL of H_2O_2 (Sigma-Aldrich, Catalogue no. H1009-500ML, 30%) were added and the mixture was incubated at 37 °C on a thermo-shaker for 1 h. After incubation, the absorbance was measured at 536 nm and the scavenging percentage of $HO^{\bullet}$ was calculated with the equation (5):

$$Scavenging\ rate\ (\%) = [(As - A1)/(Ao - A1)] \times 100 \quad (5)$$

where A_S is the absorbance of the sample; A_0 is the absorbance of distilled water in reaction and A_1 is the absorbance of hydrogen peroxide in reaction [20].

2.9.4. Superoxide Anion Radical ($O_2^{\bullet -}$) Scavenging Activity

The samples' superoxide anion radical ($O_2^{\bullet -}$) scavenging activity was determined after Petreni et al. [21] as follows: 40 µL of each sample, AA, Trolox or ethanol as negative control, was mixed with 1.8 mL Tris-HCl (TRIS base, Sigma-Aldrich, Catalogue no. 10708976001, ≥99.9%, HCl, Roth, Catalogue no. NH53.3, 35%) (0.05 M, pH 8) and incubated 20 min at 25 °C. Next, 160 µL of pyrogallol (Sigma-Aldrich, Catalogue no. 16040-100G-R, ≥99%) (25 mM) was added and the mixture was incubated at 25 °C for 5 min. In order to complete the reaction, 10 µL HCl (Roth, Catalogue no. NH53.3, 35%) (8 M) was added and the absorbance was measured at 325 nm, then the scavenging percentage was calculated using the equation (6):

$$Scavenging\ rate\ (\%) = (1 - As/Ao) \times 100 \quad (6)$$

where A_0 is the control's absorbance and A_S is the sample's absorbance [21].

2.9.5. Ferrous Ions' (Fe^{2+}) Chelating Activity

The chelating activity of the samples was compared to AA and Trolox (as common antioxidant references) and was estimated using a previously described method [20] as follows: 200 µL of each sample, AA, Trolox and ethanol as negative control, and 100 µL ferrous chloride tetrahydrate (Sigma-Aldrich, Catalogue no. 157740-100G, ≥97%) (2 mM) were mixed. In addition to these, 200 µL ferrozine (Sigma-Aldrich, Catalogue no. 82950-1G, ≥97%) (2 mM) was added and the total volume was adjusted to 2 mL with ethanol (Sigma-

Aldrich, Catalogue no.459844-4X2.5L, ≥99.5%). The mixture was incubated at room temperature for 10 min, then by measuring the absorbance of the Fe^{2+}-ferrozine complex at 562 nm, the Fe^{2+} chelating activity was estimated using the equation (7):

$$Fe^{2+}\text{chelating effect}\ (\%) = (1 - As/Ao) \times 100 \qquad (7)$$

where A_0 is the control's absorbance and A_S is the sample absorbance.

2.9.6. Ferric Ions (Fe^{3+}) Reducing Antioxidant Power (FRAP) Assay

FRAP assay was performed using a protocol adapted and published previously [20], as follows: 50 µL of all the studied samples, AA, Trolox or ethanol as negative control, was mixed with 650 µL sodium phosphate buffer (Na_2HPO_4 (Chemical, p.a.) /KH_2PO_4 (Chemical, p.a.), 0.2 M, pH 6.6) and 650 µL 1% potassium ferricyanide (Merk, Catalogue no. 1049730100, p.a.) and the mixture was incubated for 20 min at 50 °C. After 20 min, 650 µL trichloroacetic acid (Chempur, Catalogue no. 115779700, p.a.) (10%) was added to the mixture and 910 µL of this solution was mixed with 910 µL distilled H_2O and 180 µL ferric chloride (VWR Chemicals, Catalogue no. 24127237) (0.1%). The absorbance was measured at 700 nm. The reducing power (%) was expressed as the ratio between the sample absorbance and the blank absorbance.

2.9.7. Lipid Peroxidation Inhibitory Assay

Lipid peroxidation inhibitory activities were measured by a previously described method [20] as follows: 100 µL of each sample, AA, Trolox or ethanol was mixed with 900 µL phosphate buffer (0.2 M dipotassium hydrogen phosphate (Lach-Ner), pH 7) and 1000 µL linoleic acid emulsion. The emulsion was prepared by mixing 175 µg Tween-20 (Sigma-Aldrich, Catalogue no. P1379-25ML, ≥40%) and 155 µL linoleic acid (Sigma-Aldrich, Catalogue no. W800075-100G, ≥95%) in 50 mL phosphate buffer (Lack-Ner) 0.2 M). The mixture was incubated at 37 °C and 50 µL of this solution were taken after 1h and then after 24 h, mixed with 1.85 mL ethanol (Sigma-Aldrich, Catalogue no.459844-4X2.5L, ≥99.5%) and 50 µL $FeCl_2$ (VWR Chemicals, Catalogue no. 24127237) solutions (20 mM in 3.5% HCl (Roth, Catalogue no. NH53.3, 35%)), mixed vigorously then 50 µL of potassium thiocyanate (Supelco, Catalogue no. 1051250250, p.a.) (30%) was added. The absorbance of the resulting clear solution was recorded at 500 nm, and the inhibitory effect was calculated using the equation (8):

$$Inhibition\ effect\ (\%) = (1 - As/Ao) \times 100 \quad (8)$$

where A_S is the absorbance of the sample and A_0 is the control's absorbance [20].

2.10. Statistical analysis

Statistical analysis was performed with the GraphPad Prism 8 software (GraphPad Software Inc., San Diego, CA, USA). Experimental data (AV, PV, antioxidant properties) were represented as means ± standard deviation. Results for AV and PV were analysed by paired or independent two-tailed (Student's) *t*-test, compared to SFO (to assess the effect of ozonation time) or to 0M (to assess the effect of storage conditions). For antioxidant activity data, all samples were compared to AA or SFO using One-way ANOVA with Dunnett's test for multiple comparisons. In the case of lipid peroxidation inhibitory assay, the results were analysed by Two-way ANOVA with Dunnett's test for multiple comparisons (vs. AA or vs.

SFO) or by multiple t-tests using the Holm-Sidak method, with alpha = 0.05 (1h vs. 24h). Adjusted p-values are presented in Tables S5 and S6. For all statistical analysis, $p < 0.05$ was considered statistically significant (95% confidence interval).

3. Results and discussions

3.1. Experimental design and samples codification

This study aimed to produce a natural, organic SFO with high curative potential through ozonation, without any other chemical modifications. Sunflowers were grown without the use of fertilizers or insecticides (organic conditions), and the resulting seeds were dried and cold-pressed to obtain raw SFO, which was stored at 8 °C in hermetically sealed glass containers to prevent degradation. Vegetable oils are generally susceptible to oxidation, a process that negatively affects their physical and chemical properties [5]. However, ozonation can significantly extend the shelf life of oils while also enhancing their therapeutic properties [13].

To develop a SFO with curative properties, the oil was subjected to ozonation for 12 hours. To monitor the ozonation degree, samples were extracted every 2 hours using an oil syringe (the sample coding is detailed in Table S1). The SFO before ozonation was considered the control sample. Additionally, an SFO-water emulsion was prepared in a precise ratio of 9:1 (w/w) and thoroughly homogenized until a uniform emulsion was achieved. The resulting emulsions were also ozonated under identical conditions mentioned above, for 12 hours, and samples were taken every 2 hours for analysis (see Table S1 for coding). Also, SFO-water emulsion before ozonation was considered as control sample.

To evaluate the stability of both ozonated SFO samples (in SFO and SFO-water emulsion forms), the resulting samples after 12 hours of the ozonation process were stored at room temperature (approximately 24 °C), as well as refrigerated (4 °C) for 6 months. In parallel, raw SFO and SFO-water emulsion which were stored at 8 °C for 6 months were subjected to the same ozonation procedures to assess the reproducibility of the ozonation process using the same raw initial SFO.

3.2. Acid value (AV) of ozonated SFO

The acidity of vegetable oils is a critical parameter, that serves as an indicator of degradation by-products which may result during the ozonation process [22]. At the same time, an AV below 1 indicates the superior nutritional quality of SFO [3]. According to published literature, ozonation modifies the chemical structure of the oil's components, leading to the formation of new compounds [13]. In the case of SFO, it is expected that the acid index increases with longer ozonation times, primarily due to the oxidation of carbonyl groups by the excess ozone. Aside from acid value (AV), other physico-chemical properties of vegetable oils, such as peroxide value (PV), density, and viscosity, are also influenced by the ozonation degree [13].

Figure 1 illustrates the AV results obtained for all samples. Figure 1a and 1c illustrate the graphical representation of AV as a function of ozonation time for both SFO and SFO-water emulsion. Figures 1b and 1d display the AV differences over time, relative to the 0-hour ozonation sample (SFO), which was arbitrarily assigned a value of 1 for comparison purposes.

In Figure 1, the blue curve represents the AV obtained for samples that were subjected to ozonation as soon as the oil was obtained, the orange curve represents the AV obtained for the two samples that were kept at room temperature for 6 months, the green curve represents the AV obtained for the oil sample that was stored at 8 °C and then subjected to ozonation both as oil and as emulsion.

Following the blue curves in Figures 1a and 1c (0M), both sample types (SFO and SFO-water emulsion) exhibit minimal changes in AV during the first six hours of ozonation, with only slight increases observed by the end of the 12-hour process (Table S2). After storage of samples at room temperature for six months (orange curve, 6M), the determined AV indicate an acid stability for SFO samples ozonated for up to 6 hours, as reflected in Figure 1b. Nevertheless, we can observe that the AV increases significantly over ozonation time and storage duration, from 0.778±0.001 to 3.073±0.015 mg NaOH/g oil for SFO and from 1.518±0.019 to 7.488±0.066 mg NaOH/g oil for SFO after 6 months storage. We can observe these differences also for SFO-water emulsion, where we recorded values from 1.382±0.005 to 3.280±0.028 mg NaOH/g oil for SFO-water emulsion and from 2.031±0.092 to 10.162±0.155 mg NaOH/g oil for SFO-water emulsion after 6 months storage (Table S2). Figures 1b and 1d show a progressive increase in AV as a function of ozonation time for both oil and oil-water emulsion samples, with the most pronounced differences observed in oil-water emulsion samples (Figure 1d and Table S2)). On the other hand, if we observe the blue and green columns in Figures 1b and 1d and Table S2, we can see that the reproducibility of the experiment is high, as the values are very similar, indicating consistent results across different storage conditions, regardless if the SFO was used immediately or stored for 6 months at 8 °C and then ozonated.

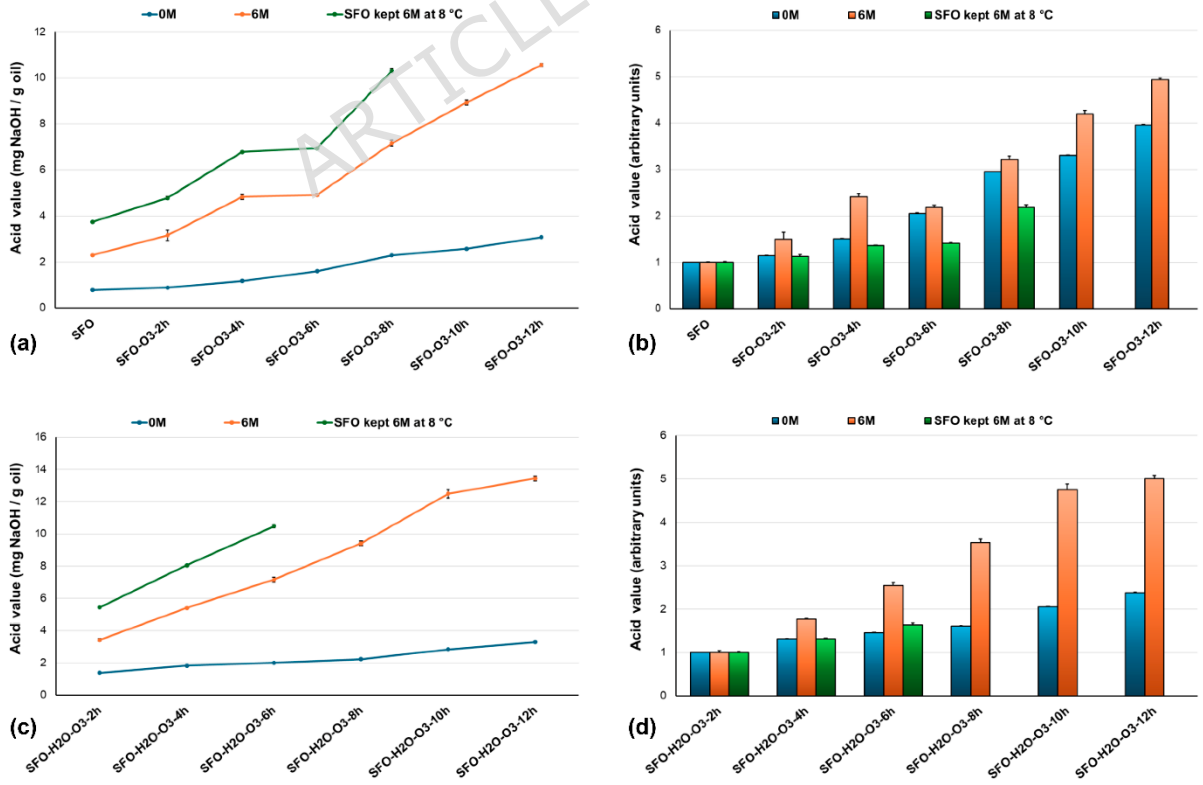

Fig. 1 The variation of acid values (AV) as a function of ozonation time and storage duration: **(a)** ozonated SFO; **(b)** AV differences over time for ozonated SFO, relative to the 0-hour

ozonation sample (SFO), with arbitrarily assigned value of 1 for comparison purposes; **(c)** ozonated SFO-water emulsion; **(d)** AV differences over time for ozonated SFO-water emulsion, relative to the 0-hour ozonation sample (SFO), with arbitrarily assigned value of 1 for comparison purposes.

However, when comparing the starting AV in Figures 1a and 1c and Table S2, we observed that the AV for the oil stored at 8 °C for 6 months and then ozonated (green curve) is higher than that of the oil ozonated then stored at room temperature. This suggests that even under low-temperature storage, some raw SFO degradation occurs, increasing the initial AV. Nevertheless, the conclusion is that ozonation effectively preserves the oil's properties under both storage conditions, maintaining stability and preventing significant deterioration over time. Our results are confirmed by another study which showed that rapeseed or flaxseed oils are better preserved when ozonated, preventing the formation of secondary compounds resulting from the oxidation of phytosterols from the oil composition [2].

The SFO ozonated for 12-hours (SFO-O_3-12h-6M4°C) and the SFO-water emulsion ozonated for 12-hours (SFO-H_2O-O_3-12h-6M4°C) were stored at 4 °C for 6 months. Then, the samples were analysed further to compare the effect of different storage conditions on their acid stability. In this context, as shown in Table S2, the AV of the ozonated SFO remained virtually unchanged after six months, indicating high acid stability, from 3.073±0.015 to 3.723±0.081 mg NaOH/g oil. In contrast, the AV of the ozonated SFO-water emulsion was higher but still approximately half the value observed in the same emulsion stored at room temperature with recorded values from 3.280±0.028 to 5.721±0.081 mg NaOH/g oil. These results suggest that storage at 4 °C effectively preserves the AV stability of ozonated SFO samples, minimizing the acid modification over time.

3.3. Peroxide value (PV) of ozonated SFO

Peroxide value (PV) is commonly used as a key indicator of the ozonation process and serves as an important measure for evaluating the stability of ozonides in vegetable oils. This assessment is crucial for determining optimal storage conditions and ensuring product stability during commercial distribution [7].

Figure 2 shows the graphical representation of PV results, the same as described above for AV. Figure 2a and 2c depict the PV of ozonated SFO and SFO-water emulsion over time. Samples subjected to ozonation for up to 6 hours show a stable PV over 6 months, followed by a slight increase, with recorded values from 1262.76±63.41 to 1505.82±74.29 mmol/equiv/g oil for SFO sample and from 1386.78±69.43 to 1434.27±71.17 mmol/equiv/g oil for SFO-water emulsion sample. Additionally, SFO stored at 8 °C prior to ozonation exhibited a higher PV compared to oil ozonated immediately after cold-pressing.

SFO-water emulsion samples had an initial PV more than two-fold higher (Figure 2b, Table S2), yet followed a similar upward trend, maintaining high PV stability even after 6 months of storage (Figure 2d). While the PV generally increases over storage time, it remains relatively stable, indicating the long-term PV stability of ozonated vegetable oils, whether in the form of crude oil or emulsion.

In other words, the higher the PV is, the more ozone is bound in the oils structure. At the same time, a high PV value means that these samples have high potential for significant

antimicrobial capacity. Putting these conclusions together, we can say that our samples are perfect candidates for testing against microbial strains resistant to current treatments, exhibiting high potential of having significant therapeutic properties.

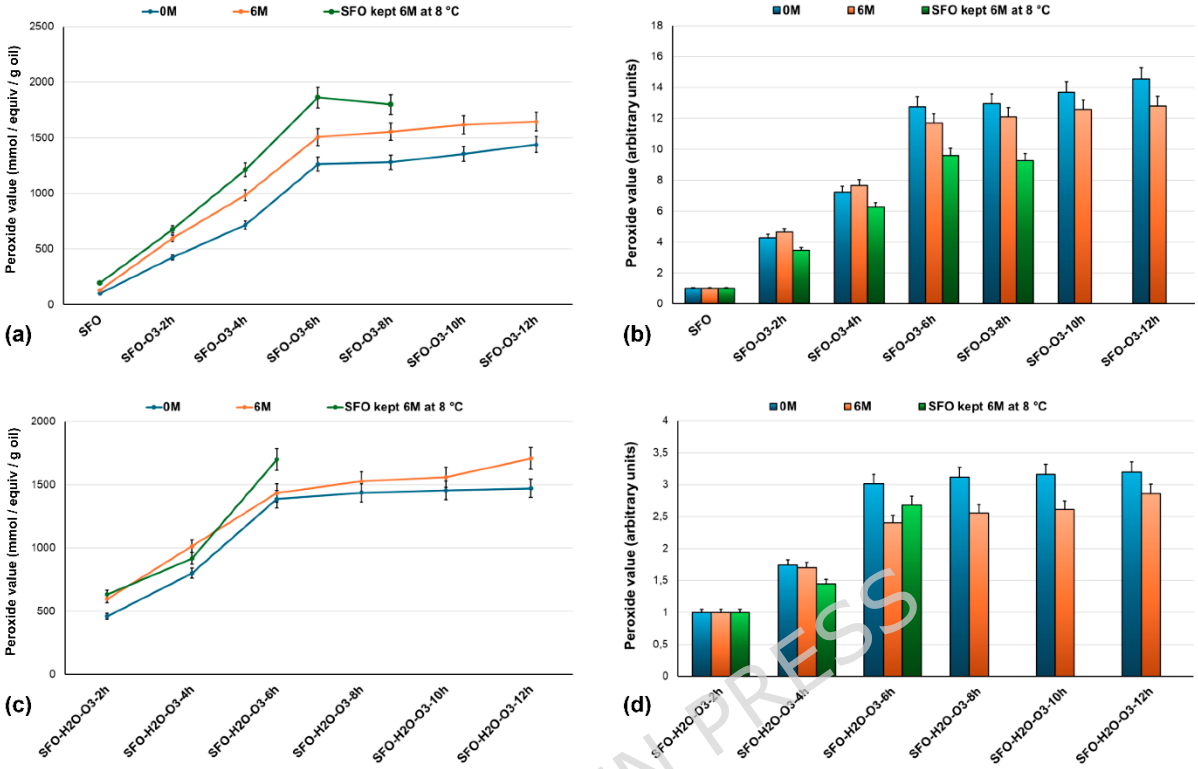

Fig. 2 The peroxide value (PV) analysis for all studied samples. **(a)** PV for ozonated SFO; **(b)** PV variation versus ozonation time for ozonated SFO, relative to the 0-hour ozonation sample (SFO), with arbitrarily assigned value of 1 for comparison purposes; **(c)** PV for ozonated SFO-water emulsion; **(d)** PV variation versus ozonation time for ozonated SFO-water emulsion, relative to the 0-hour ozonation sample (SFO), with arbitrarily assigned value of 1 for comparison purposes.

3.4. Rheological behaviour of ozonated SFO

The dependence of shear viscosity as a function of shear rate is given in Figures 3a and b for two representative samples, SFO and SFO-H_2O-O_3-8h for temperatures ranging from 0 °C to 100 °C. SFO behaves as a Newtonian fluid at all investigated temperatures, the viscosity decreases as the temperature increases. For the ozonated oils, at a given temperature, the viscosity increases as compared with SFO, due to stronger intermolecular interactions in the new formed species (ozonides and oligomers of ozonides), in agreement with previous data reported in literature [23,24]. For the investigated range of shear rates, the Newtonian behaviour was observed only above 25 °C. Below 25 °C, the viscosity depends on the applied shear rate and a complete flow curve is registered. At low $\dot{\gamma}$ values (below 10^{-2} s^{-1}), the rest state is not disturbed, and shear forces are not able to overcome the intermolecular interactions. By further increase of $\dot{\gamma}$, the oils' molecules start to orient along the flow direction and the viscosity scales as $\dot{\gamma}^{-0.6}$ (non-Newtonian behaviour). Above 10 s^{-1}, the viscosity becomes independent of the applied shear rate and the second Newtonian region is reached.

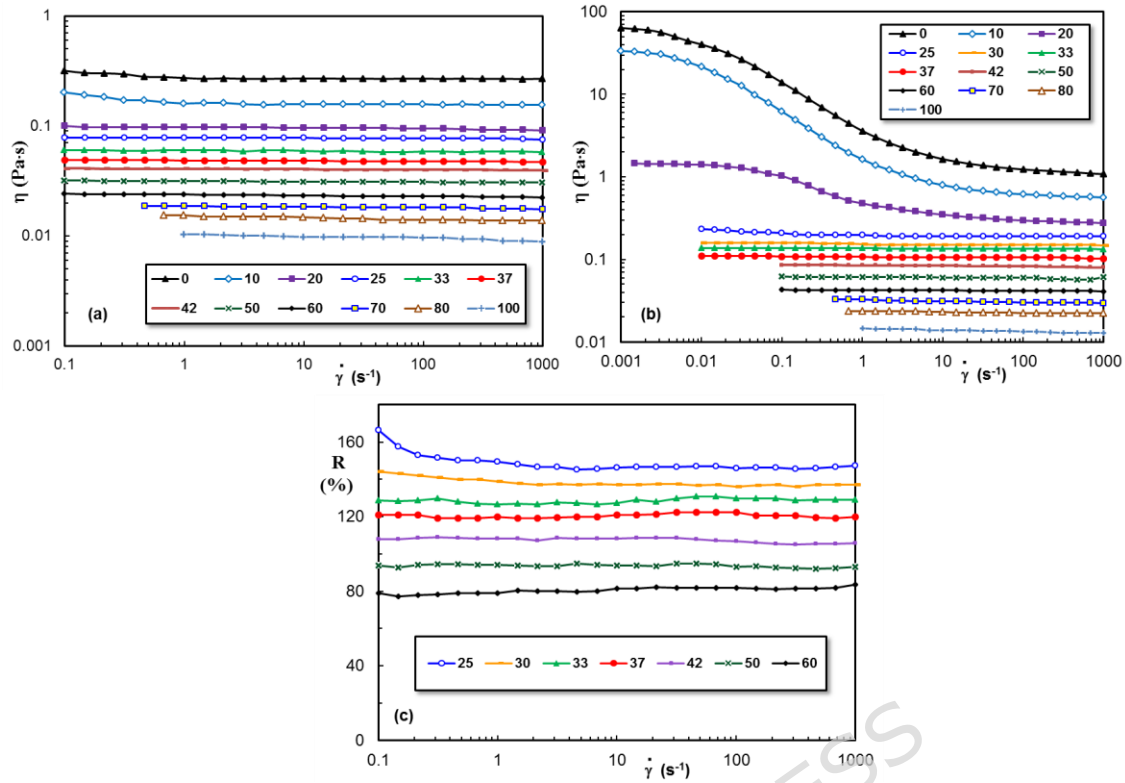

Fig. 3 The shear viscosity as a function of shear rate for **(a)** SFO and **(b)** SFO-H_2O-O_3-8h at different temperatures; **(c)** changes in the apparent viscosity of SFO-H_2O-O_3-8h induced by ozonation in the range 25 °C – 60 °C.

At 20 °C, the value of Newtonian viscosity increases from 97.4 mPa·s to 1370 mPa·s; at higher temperatures, the difference in viscosity before and after ozonation becomes smaller, as for example from 48.5 mPa·s to 107.4 mPa·s at 37 °C. This suggests that the stronger intermolecular interactions occur at low temperatures (up to 20 °C) for ozonated oil samples and at higher temperatures their intensity is diminished. However, even by heating at 37 °C, the viscosity value exceeds the double of the initial viscosity registered before the treatment. In addition, the ozonated high-oleic sunflower is a stable product, after 12 months the viscosity values are almost unchanged.

The conversion of double bonds from fatty acids into ozonated chemical species with larger size (ozonides and oligomers of ozonides), is accompanied by a viscosity increase. In addition, by introducing new polar groups, intermolecular interactions are established through O•••H hydrogen bonding and O•••O contacts. These interactions, along with dipole-dipole forces from the polar ozonides, contribute to intermolecular forces in ozonides.

According to the experimental data, we can conclude that the flow behaviour for ozonated oil samples (SFO-O_3-8h and SFO-H_2O-O_3-8h) is very similar, but their viscosity and flow activation energy increase as compared with SFO. The viscosity value is influenced by the ozonation time, and it was previously shown that the oil viscosity becomes higher as the ozonation time increases [25].

Rheology is considered a useful tool in providing a rapid quality control assessment during the entire ozonation process, as well as for determining the optimal process time for obtaining the desired ozonation level of the sample [23]. The evaluation of vegetal oils' viscosity allows an estimation of the presence of double bonds in the samples. Thus, it is

expected that ozonation of oils will be accompanied by an increase in viscosity due to the disappearance of double bonds. As ozonation time increases, higher molecular weight compounds are formed and the total unsaturation is diminished. The increased shear viscosity and peroxide values reflect the structural changes in the oil during ozonation. Similar behavior was reported previously, the viscosity of sunflower oil increased after ozonation [23]. The oil composition and the ozonation degree influences the formation of various species: iso-ozonides, inferior oligomers of ozonides (dimers, trimers) or polyperoxides. Higher unsaturation and longer ozonation times favor the formation of these complex products, while initial ozonation primarily yields ozonides. Different oils react differently based on their fatty acid profile, affecting the specific types and rates of reaction [23,25].

In order to quantify the changes in the apparent viscosity of oil by ozonation, the following ratio was calculated:

$$R = \eta SFO\ ozonated - \eta SFO/\eta SFO \quad (8)$$

Figure 3c shows the dependence of parameter R on $\dot{\gamma}$ values for different temperatures in the range 25 °C – 60 °C, covering the biomedical applications. The highest effect was registered at lower temperatures (Figure S2). At 37 °C, the viscosity increases is about 120%. In addition, the ozonated high-oleic sunflower is a stable product, after 12 months the viscosity values are almost unchanged.

The activation energy of flow (E_a) can be calculated according to an Arrhenius-type equation (9):

$$\eta = Aexp(Ea/RT) \quad (9)$$

where A is a pre-exponential factor, R is the universal gas constant, 8.314 J/(mol·K), and T is the absolute temperature (K).

By plotting lnη as a function of 1/T, two linear dependences are described by experimental data (Figure S1) and E_a was calculated the two corresponding temperature ranges (Table S3). Above 33 °C, the oils' flow activation energy values increase after ozonation and are slightly higher for sample SFO-H_2O-O_3-8h as compared with SFO-O_3-8h. However, in the region of low temperatures, E_a increases more than three times for oil samples submitted to ozonation.

The ozonation degree was correlated with the total unsaturation. The viscosity increase during ozonation of sunflower oil is associated with the formation of higher molecular weight compounds. Ozone reacts with the double bonds in fatty acids, creating ozonides and polyperoxides. These compounds are larger and more complex molecules as compared to the original fatty acids. As a consequence, the resistance to flow increases, leading to a significant rise in the overall viscosity. The gradually conversion of double bonds in fatty acids into ozonides and polyperoxides (oligomeric ozonides) with larger size is accompanied by a viscosity increase, reflected by parameter R.

3.5. NMR analysis

3.5.1. NMR analysis of native SFO

The proton NMR spectrum associated with native high-oleic (C18:1) SFO is included in Figure 4. From previous experience in NMR analysis of different vegetable oils [26,27], the eight signals visible in the proton spectrum can be associated with the following groups

present in fatty acids: triplet centred at 0.86 ppm is generated by the terminal methyl protons from all acids except linolenic; multiplet in the interval 1.24-1.28 ppm corresponds to methylene protons from all fatty acids chains; broad signal centred at 1.59 ppm belongs to methylene protons in β position relative to carboxylic groups from all fatty acids; multiplet in the interval 1.98-2.00 ppm corresponds to methylene protons in α position relative to double-bond groups from all unsaturated fatty acids; triplet centred at 2.29 ppm is generated by the methylene protons in α position relative to carboxylic groups from all fatty acids; triplet centred at 2.75 ppm belongs to methylene protons between the double-bonds from linoleic acid; the two doublet of doublets resonating in the interval 4.10-4.30 ppm are assigned to glycerol protons in positions 1,3; the complex signal visible in the interval 5.22-5.33 ppm is generated by both methynic protons in position 2 from glycerol and olefinic protons from all unsaturated fatty acids. Because the SFO used in this study was obtained from high-oleic sunflower seeds, the proton NMR signal associated with linoleic acid (C18:2) from 2.75 ppm (annotated with F in Figure 4a) is significantly less intense compared with the same signal in commercially available SO.

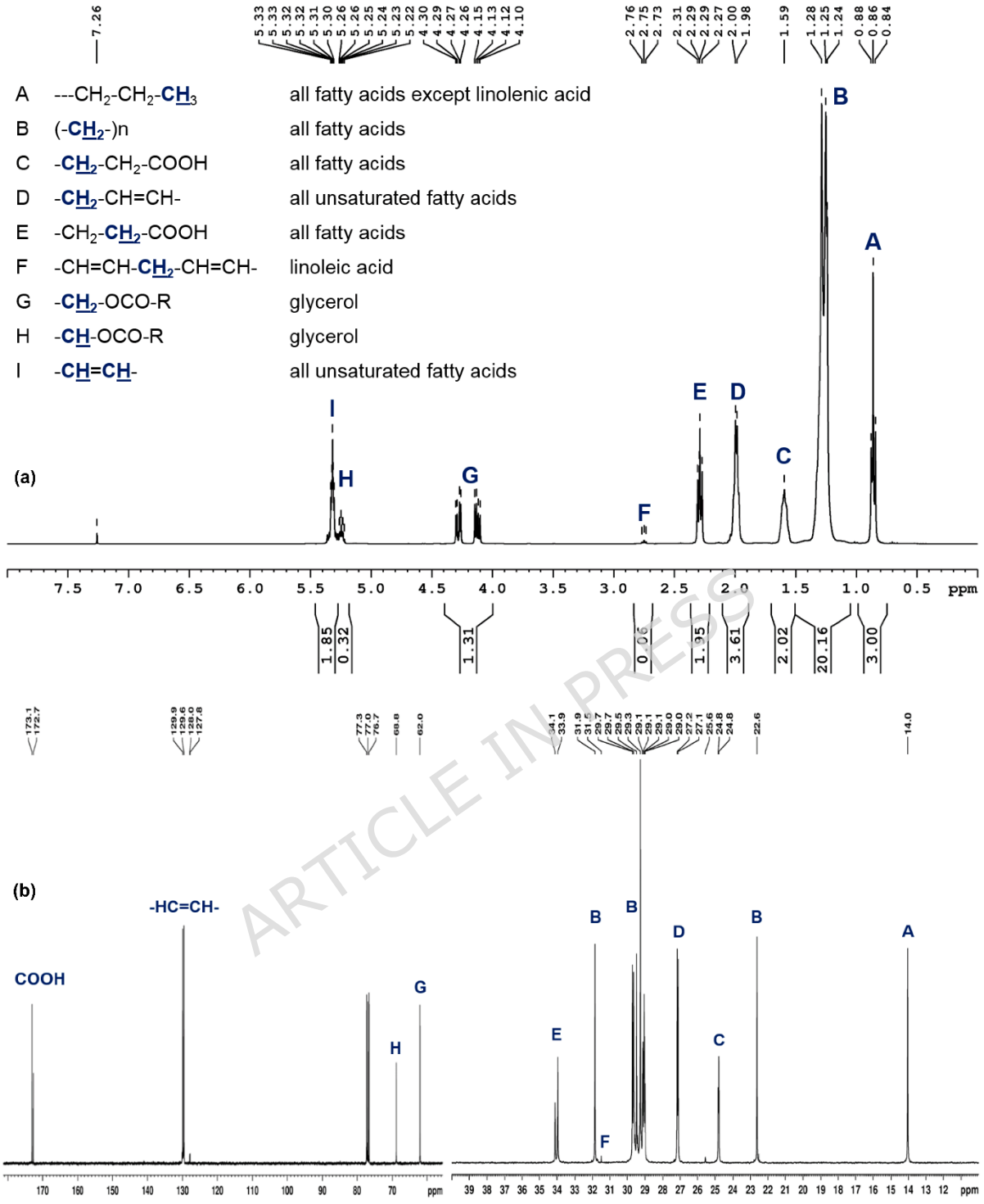

Fig. 4 (a) The ^{1}H-NMR spectrum corresponding to native SFO, recorded in $CDCl_3$, at 400 MHz; **(b)** The ^{13}C-NMR spectrum corresponding to native SFO, recorded in $CDCl_3$, at 100 MHz. The signals' assignments are annotated on the figure.

Introducing the integrals' values in the previously developed chemometric equations [26] we were able to establish the composition of our SFO in terms of linoleic, mono-unsaturated and saturated fatty acids. Thus, for this particular oil sample, maintaining *x*, *y*, *z* and *t* as the molar ratios of linolenic, linoleic, mono-unsaturated (oleic acid) and saturated fatty acids, the first chemometric equation accounting for the sum of the molar ratios equals

1: $x + y + z + t = 1$ becomes $y + z + t = 1$, since no linolenic acid is present in our oil sample ($x=0$).

The molar ratio of linoleic acid (y) is obtained from the equation: $y = \frac{I_F - 4kx}{2k}$, where k is a coefficient that correlates the signal integral with the number of protons that signal is due to and can be determined from $k = \frac{I_C}{2}$, as described in the initial study [26]. Replacing the integrals' values in the above equations, we obtain the molar ratio of linoleic acid (y) of 0.03.

The molar ratio of mono-unsaturated fatty acids (z) is obtained from the equation: $z = \frac{I_D - 4ky}{4k}$, giving 0.89 after replacing the integrals' value.

The saturated fatty acids molar ratio (t) is obtained from the difference $1-y-z$, resulting 0.08. Consequently, we can conclude that our SFO sample contains 3 % linoleic acid, 89 % mono-unsaturated fatty acids (i.e. oleic acid) and 8 % saturated fatty acids, results confirmed by literature data [4].

The composition of all oil samples, obtained from the chemometric equations, using the proton integrals' values, is listed in Table S4. According to literature data [3], unsaturated and polyunsaturated acids promote the oxidation process through the reaction of hydrogen atoms from linoleic acid with atmospheric oxygen and the formation of peroxyl radicals. By this chemical process, free radicals are formed on the linoleic acid chain [3]. Under these conditions, if we look at the values in the composition of crude oil, we can observe that in six months it decreases from 89 to 87.9% (see Table S4). This difference can be explained by the formation of free radicals that lead to the natural oxidation of oils.

The signals present in the carbon spectrum of SFO can be rationalized as: aliphatic carbons from all saturated and unsaturated fatty acids in the region 13.0-35.0 ppm (annotated A to F in Figure 4b), glycerol -CH_2- at 62.0 ppm, glycerol -CH- at 68.8 ppm (annotated G and H in Figure 4b), unsaturated CH carbons between 127.0 and 130.0 ppm and carboxyl groups from 172.0 to 174.0 ppm [27]. In the particular case of our high-oleic oil, the low amount of linoleic acid is indicated by the very low intensity signals from 25.6 and 31.5 (-CH_2-), 127.8 and 128.0 ppm (-CH=CH-).

We also checked through NMR spectroscopy the stability of the oil sample after being kept at 8 °C for 6 months. The proton and carbon NMR fingerprints were very similar with those of the initial oil sample. Applying the same chemometric equations, we obtained a composition of 3 % linoleic acid, 87 % mono-unsaturated fatty acids and 10 % saturated fatty acids. This only 2 % difference can be correlated with experimental errors like sample homogeneity, manual spectral processing in terms of signals phase adjustment and baseline correction, and even from manual signals' integration.

3.5.1. NMR analysis of ozonated SFO

The NMR profile of ozonated vegetable oils has been described in the literature [14,28–31]. However, we did not find any references on ozonated SFO characterized through NMR spectroscopy.

After 2 hours of reaction with ozone, we were able to identify new signals in the proton spectrum of the ozonated SFO. These signals increase over time and, based on

previous studies [28–31], they can be assigned to compounds containing 1,2,4-trioxolane rings, hydroxy-hydroperoxydes and aldehydes, as exemplified in Figure 5. These assignments were also verified in bidimensional proton-proton and proton-carbon correlation experiments like H, H-COSY and H, C-HSQC.

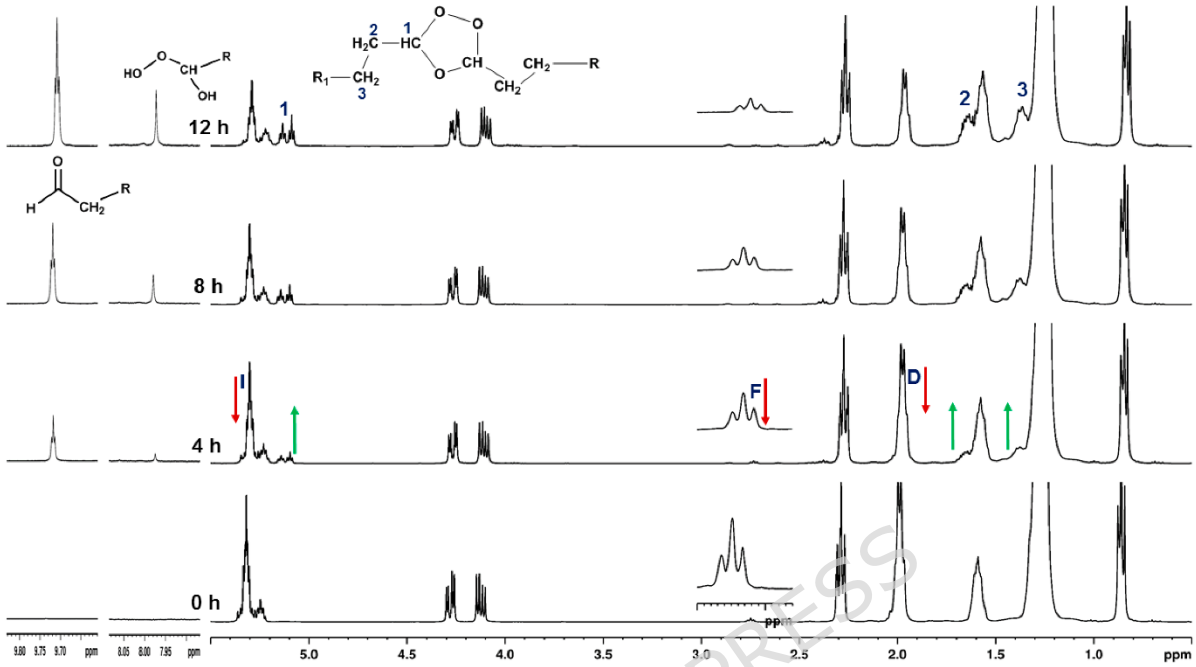

Fig. 5 The variation of proton NMR pattern for the SFO ozonated for 4, 8 and 12h, compared with the native oil, recorded in $CDCl_3$, at 400 MHz. The signals' assignments are annotated on the figure.

The rest of the proton signals are those described and assigned for the native SFO (Figure 4a). A significant difference is observed in the intensities (integrals) of the signals associated with unsaturated fatty acids (i.e. linoleic and oleic acids), mainly those from 1.94-1.97 ppm (signal D), 2.71-2.74 ppm (signal F) and 5.28-5.31 ppm (signal I). These three signals are less intense (smaller integrals' values) as the ozonolysis reaction develops in time, the ozone acting upon the double bond according with Criegee's mechanism [28] (see Figure 5 and Figure S3).

The gradual formation of these compounds, accompanied by the consumption of the unsaturated bonds, was monitored using the protons' integrals, as exemplified in Figure S1. Thus, in the first 4 hours of the reaction with ozone, the unsaturated bonds decrease by 20%, reaching almost 54% after 12 hours of reaction. By the end of the reaction, the major oxygenated product were ozonides derivatives, which were formed almost in tandem with the decrease of the unsaturated protons signal from 5.30 ppm. The ratio between ozonides and aldehydes seemed to be constant throughout the ozonation reaction, with five times less aldehydes and trace amounts of hydroxy-hydroperoxydes (Figure S3). Almost 46% of the initial high-oleic sunflower oil remains unreacted.

The NMR signals for the newly formed ozonation products are clearly visible in the proton spectrum of high oleic sunflower oil ozonized for 12h (Figure 5, top spectrum).

The presence of 1,2,4-trioxolane rings is indicated by the two triples centred at 5.09 and 5.13 ppm (signals annotated with 1 in Figure 5; δ_{13C} = 103.99 to 104.17 ppm) that display

spin-spin couplings in COSY spectrum (Figure S4) with methylene protons from 1.62-1.66 ppm (signals annotated with 2 in Figure 5; δ_{13C} = 32.27, 32.22 ppm). A second correlation signal in COSY spectrum connects the methylene group with protons resonating at 1.32 ppm (signals annotated with 3 in Figure 5), highlighting the propyl residue from newly formed 1,2,4-trioxolane rings (see Figure S4).

Carbon edited experiments, like DEPT-135, and heteronuclear correlation experiments, like H,C-HSQC, were further used to confirm the proposed 1,2,4-trioxolane rings. From the proton-carbon direct correlation HSQC spectrum (Figure S5), the carbon atoms associated with the propyl residue were identified at the following chemical shifts: 23.4-23.7 ppm (CH_2-3), 30.5 and 32.1 ppm (CH_2-2) and 103.8-103.9 ppm (CH-1 from trioxolane ring, highly deshielded by the two covalently linked oxygen atoms). The distinction between CH and CH_2 groups was obtained from DEPT-135 spectrum (Figure S6) in which the two CH_2 groups from 23 ppm, 30 and 32 ppm appear on the positive side of the spectrum while the CH group from 103 ppm is displayed on the negative side.

Another new signal observed after ozonation is the most deshielded triplet from 9.71 ppm (the left-side insert in Figure 5) and its proton-coupling partner that resonates in the interval 2.30-2.34 ppm, as indicated by the cross peak observed in COSY spectrum (Figure S7 and S8). Their associated carbon atoms resonate at 43.5-43.6 ppm (CH_2) and 202.1 ppm (CHO), as indicated by the cross peaks highlighted in the proton-carbon HSQC spectrum from Figure S9, supplementary material. The presence of a protonated carbon at 202 ppm is a clear indication for newly formed formyl group.

The third specie formed after ozonation, identified only in the proton spectra, were hydroxy-hydroperoxydes derivatives. In our case, the signal from 7.96 ppm described in the literature as a marker for hydroxy-hydroperoxydes derivatives was a very low intensity, and could be followed only in the proton spectra (Figure 5, middle insert, 7.90-8.05 ppm).

In contrast with these studies [14,28–31], no homoallylic ozonides (5.50 ppm) 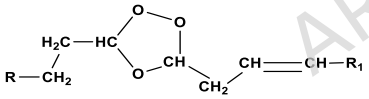 were observed in the proton spectra of our ozonated SFO. This observation is in agreement with the low content of linoleic acid, which is the main source of homoallylic ozonides due to its two unconjugated double bonds [14,30]. We did not observe significant differences when the ozonolysis reaction was performed in the presence of water (Figure 6).

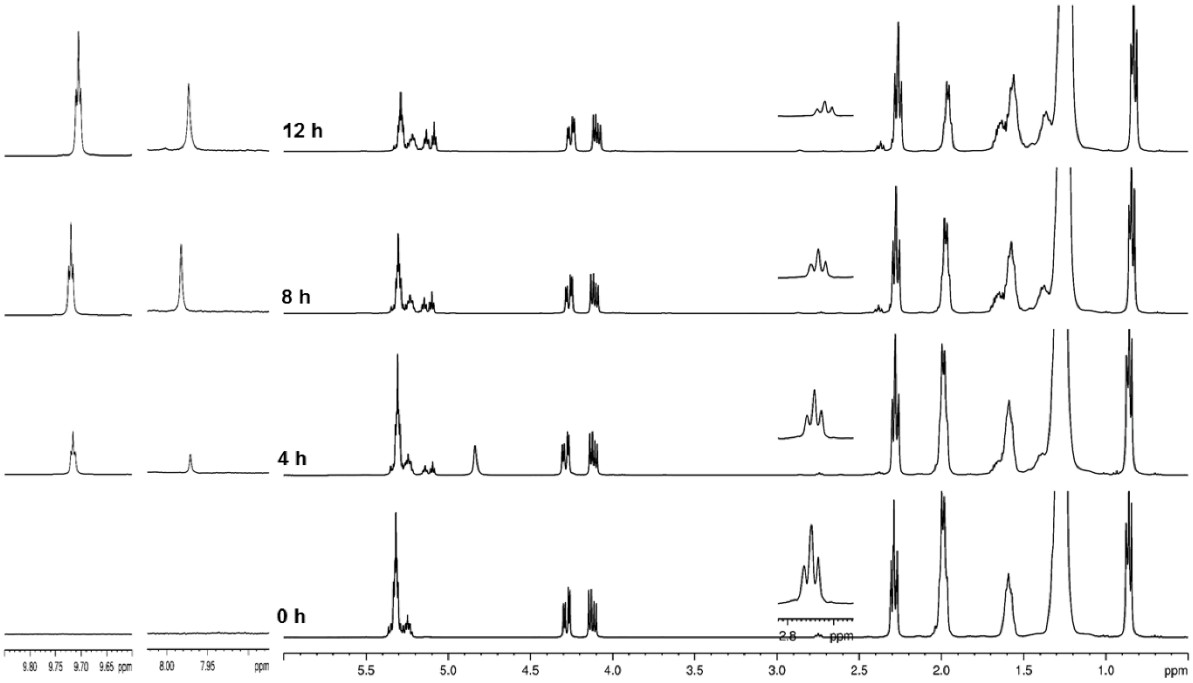

Fig. 6 The variation of proton NMR pattern for the SFO-water emulsion ozonated for 4, 8 and 12h, compared with the native oil, recorded in $CDCl_3$, at 400 MHz. The signals' assignments are annotated on the figure.

3.6. FTIR analysis of ozonated SFO

The comparative 2nd derivative of the IR spectra in the 1800-600 cm^{-1} of SFO before and after ozonation for different times of exposure is shown in Figure 7a,b,c. There are significant changes in the ozonated SFO at 2 hours and 6 hours.

The IR spectra of the ozonated sunflower oil samples have highlighted major changes in the 1722-650 cm^{-1} spectral region due to the formation of stable ozonide, trioxolane product, supporting a Criegee's ozonation mechanism by carbonyl and carbonyl oxide intermediaries. High exposure to ozone has resulted in an increase in the corresponding area of the bands at 1678, 1630, 1592 and 730 cm^{-1} attributed to trioxolane groups (Figure 7a,c), and at 1464, 1378, 1332, 1286 and 936 cm^{-1} assigned to C-H deformation vibrations confirming the cleavage of the alkene double bonds (Figure 7b).

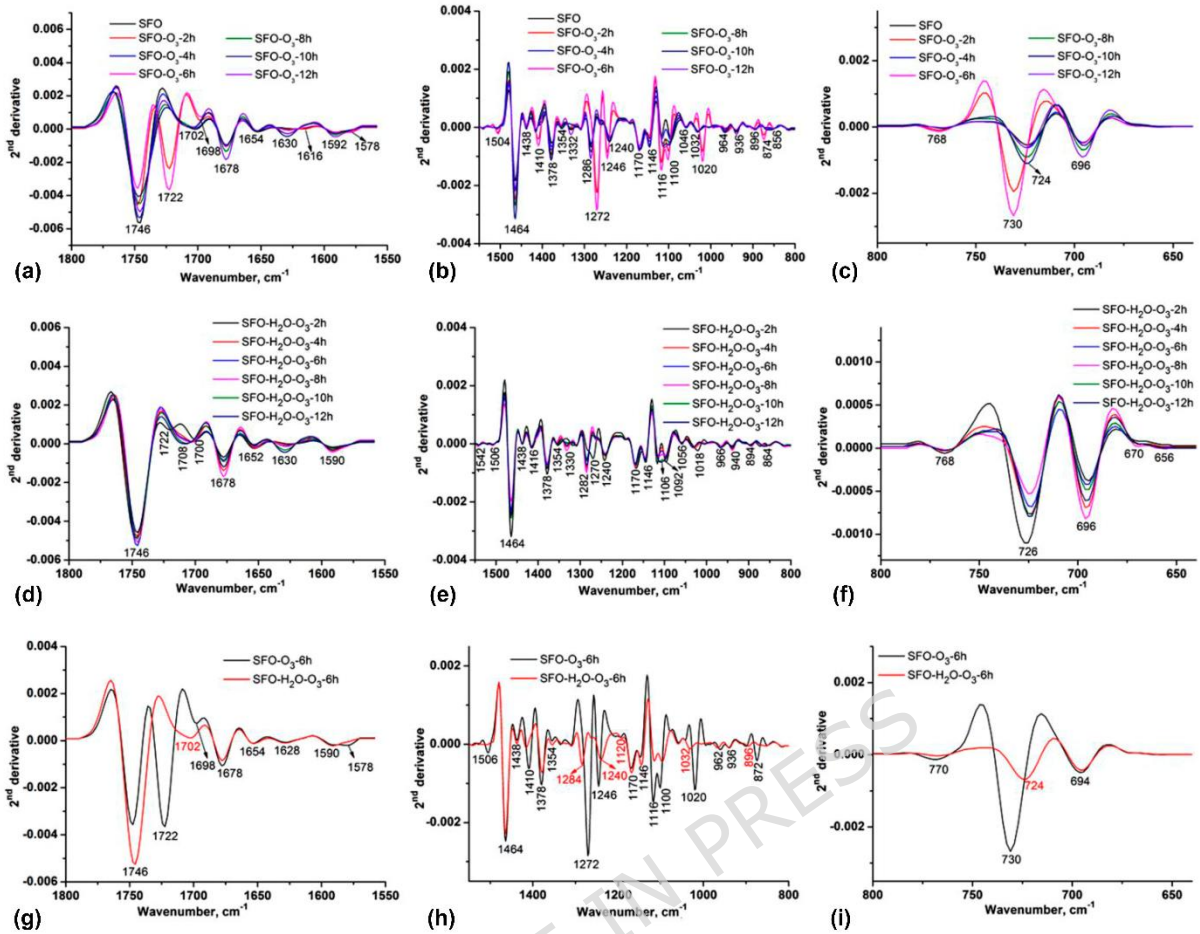

Fig. 7 The 2nd derivative of the IR spectra of SFO-O_3 and SFO-H_2O-O_3 series in the 1800-1500 cm^{-1} **(a, d)**, 1500-800 cm^{-1} **(b, e)** and 800-600 cm^{-1} **(c, f)**. The comparative 2nd derivative of the SFO-O_3-6h and SFO-H_2O-O_3-6h samples in the 1800-1500 cm^{-1} **(g)**, 1500-800 cm^{-1} **(h)** and 800-600 cm^{-1} **(i)**.

The main changes in the IR spectra of sunflower oil samples exposed to ozone and additional water also supported the ozonolysis process by the Criegee's mechanism through trioxolane group formation: decreasing in the carbonyl group at 1746 cm^{-1} area and the disappearance of the bands at 1722, 1700 and 1630 cm^{-1} (Figure 7d), blueshifting of the band at 1270 cm^{-1}, the appearance of the band at 1106 cm-1 assigned to C-O- groups after 10-12 h (Figure 7e), the area changes in the C-C skeletal bonds at 726 and 696 cm^{-1} (Figure 7f). The Criegee's mechanism involves the formation of the primary ozonide by breaking of the double group, followed by cycloaddition and retro-cycloaddition to form poly- and hydroxy peroxides, aldehydes and carboxylic acids [13].

The differences between the sunflower oil samples exposed to both, ozone and ozone with additional water, were better highlighted by 2nd derivative of the spectra after 6 h of exposure. The presence of water has resulted in accelerating ozonolysis supporting by disappearance of the band at 1722 cm^{-1} as a result of the conversion of ozonides to aldehydes and carboxylic acids confirmed by the maxima at 1678 cm^{-1}, and 1702 cm^{-1}, 1578 cm^{-1}, respectively (Figure 7g). The presence of the bands at 1100-1116 cm^{-1} (C-O stretches) has demonstrated the conversion of C=C groups into ozonides (Figure 7h), which are also visible

in the 800-600 cm^{-1} spectral region (Figure 7i) where the maxima are blueshifted in SFO-H_2O-O_3 samples due to the presence of water

3.7. Antioxidant activity of ozonated SFO

Upon reviewing the literature data on the antioxidant activity of ozonated SFOs, we observed very few studies, mostly limited to DPPH radical inhibition or ferric ion-reducing capacity assays [17]. Given this lack of comprehensive research, we chose to expand our investigation by assessing antioxidant activity using seven distinct analytical methods, providing a broader and more complementary interpretation of the results.

Among these, the ABTS and DPPH radical scavenging assays were employed because, in general, these two analysis methods complement each other. According to the results obtained from determining the DPPH radical scavenging capacity, we can observe that all samples show low inhibition capacity (Figure 8a). Furthermore, it appears that the oil-water emulsion has an even lower capacity to inhibit the DPPH radical compared to simple oil, and this activity is not influenced by the ozonation time.

Regarding the tested samples' ability to inhibit the ABTS radical, we can observe that for all the tested samples, we recorded results close to 0 or even negative (Figure 8b). This means that our samples have a very low ability to scavenge the ABTS radical or even contain groups like carbonyl oxide produced in the ozonation process, which is a highly reactive species that can potentiate the oxidising effect of the ABTS radical. This aspect is very interesting to consider if we want to enhance an oxidising effect in a neutral environment because the ABTS radical inhibition reaction takes place in a neutral environment. According to a literature study published recently by Ehsandoost et al. [32], the oxidising effect can be explained as follows: surface-active compounds from SFO, such as free fatty acids or lipid hydroperoxides, form inverted micelles in the presence of water. These structures encapsulate water, and on the outside, these hydroperoxides, which have surface activity, break down into free radicals with oxidative effects [32]. At the same time, in the ozonation process, the ozone interacts with unsaturated fatty acids containing carbon-carbon double bonds, and this interaction produces many oxygenated compounds such as aldehydes, peroxides, and ozonides with different oxidative properties [33].

Nevertheless, overall, our results are contrary to those reported in the literature. The published results have demonstrated that ozonated vegetal oils exhibit a strong scavenging activity of DPPH radicals, which is maintained over time, and is due to the oils' strong hydrophobicity [17]. These contradictory results may be explained by the fact that the literature reports tested much higher concentrations compared to our study. However, when using ozonated oils for skin applications, the concentration of the compounds that come into direct contact with the surface are in reality very low.

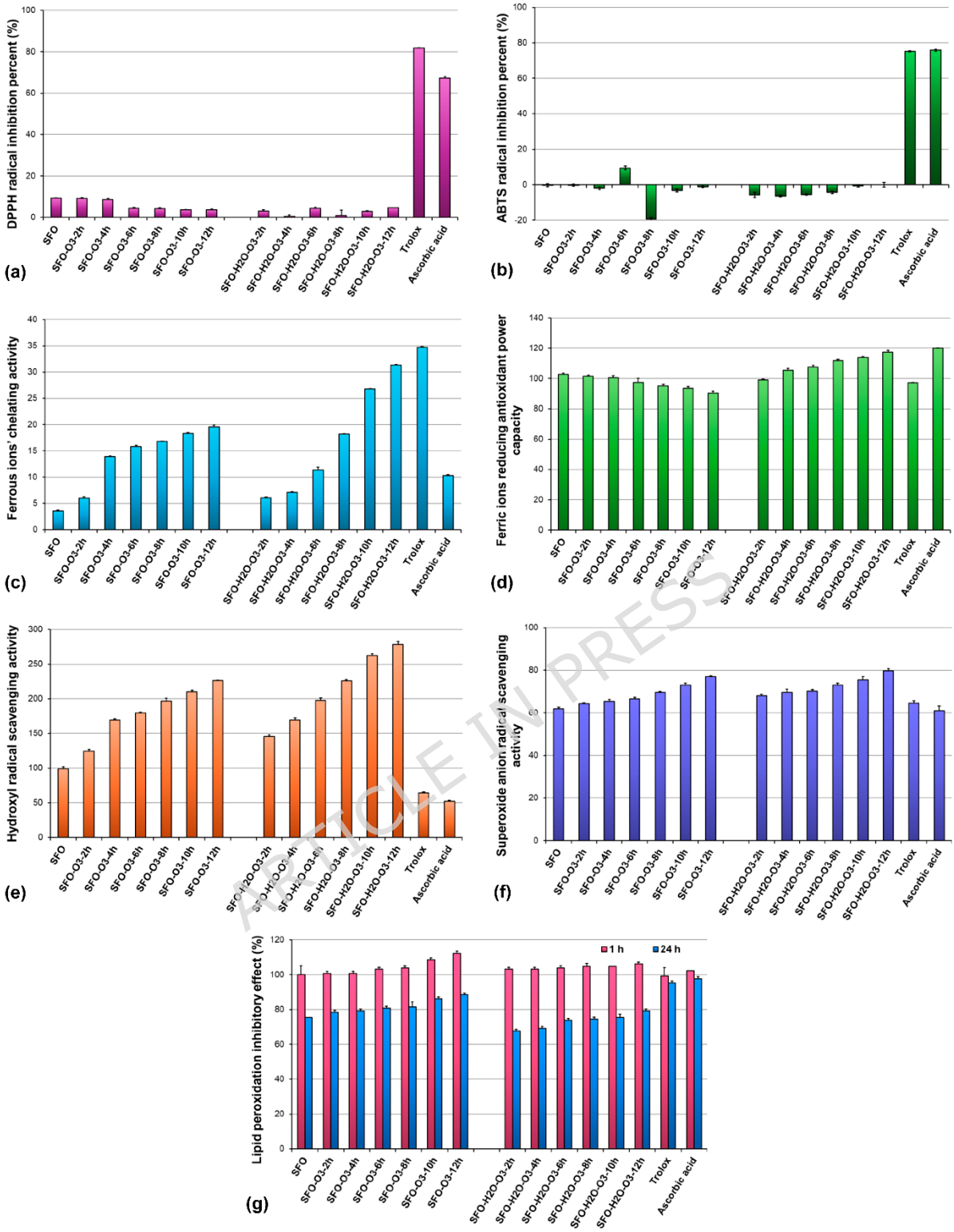

Fig. 8 The antioxidant properties of the ozonated samples: **(a)** DPPH radical scavenging assay; **(b)** ABTS radical scavenging assay; **(c)** Ferrous ions chelating activity; **(d)** Ferric ions reducing antioxidant power properties; **(e)** Hydroxyl radical scavenging ability; **(f)** Superoxide anion radical scavenging activity; **(g)** Lipid peroxidation inhibitory properties.

From Figure 8c we can observe that, as the samples' ozonation time increases, the chelating activity of ferrous ions also increases, with values recorded from below 5% for

control sample to almost 20% for SFO 12 hours ozonated sample, and from 5% to approximatively 32% for SFO-water emulsion. This aspect is correlated with ozone non-participating electrons that can bind ferrous ions, and, at the same time, the increase in chelating activity is also correlated with the increase of PV. A remarkable increase in this activity is observed for ozonated oil-water emulsions with values recorded from 5% to approximatively 32% for SFO-water emulsion. The complexing capacity of the sample ozonated for 12-hours is very close to that of Trolox. On the other hand, the FRAP capacity of the analysed samples is slightly decreased with increasing ozonation time for simple SFO (Figure 8d). In this case, we can speculate that the free reactive groups in the structures of oil components are responsible for a higher proportion of the FRAP activity of the analysed samples. In the case of emulsions, we recorded opposite values, i.e. the FRAP activity increases with increasing ozonation time, concluding that the emulsions' ozonation increases their FRAP capacity (Figure 8d). At the same time, the differences in the values recorded for all samples are not significant with increasing ozonation time, and their values are slightly higher than the Trolox FRAP value, and approach the Ascorbic Acid FRAP value. The FRAP capacity results obtained for our ozonated oils are in agreement with the data reported in the literature, showing that ozonated oils exhibit considerable antioxidant capacity and ferric ion-reducing properties [17].

The determination of hydroxyl and superoxide anion radicals' scavenging ability, as well as lipid peroxidation inhibitory properties, were performed in order to establish whether the analysed samples can neutralize free radicals and protect the cells' lipid membranes from damage. Hydroxyl radicals are the most reactive of all radicals and directly damage DNA, lipids and proteins. The superoxide anion radical is less reactive but can generate hydroxyl radicals by secondary reactions, being a precursor for the formation of other reactive oxygen species. Lipid peroxidation inhibitory activity evaluates the analysed samples' ability to prevent lipid oxidation, a process that leads to the formation of toxic products such as reactive aldehydes.

In Figures 8e, f and g, all the analysed samples show high antioxidant activity, even higher than Trolox and Ascorbic Acid. According to Sehim et al., the increased antioxidant activity correlates with the increased PV [33]. This hypothesis is confirmed by our results presented in Figures 8e and f, showing that hydroxyl and superoxide anion radicals' scavenging activity increases with ozonation time, being in correlation with the increase of PV (Table S2). The increase in PV means that in the oil structure, there are active groups with oxidizing activity that was produced as a result of ozone treatment [33]. By comparing the lipid peroxidation inhibition results, it is evident that the SFO-water emulsions present a higher activity than ozonated SFO (Figure 8g). This can be attributed to the presence of water in the system, promoting hydration of the sample and, finally, leading to an increase in lipid peroxidation capacity. This effect was observed very intensely after 24 hours of reaction time (Figure 8g).

4. Conclusions

The ozonation process preserves the SFO's AV stability and prevents significant deterioration of this indicator over time. While the PV generally increases over time, it remains relatively stable, indicating also long-term stability of PV of ozonated vegetable oils.

Due to the fact that our samples exceed a PV of 1500, they meet the conditions to be applied in biological assays targeting skin wound management.

The rheological flow behaviour for ozonated oil samples (SFO-O_3-8h and SFO-H_2O-O_3-8h) is very similar, but their viscosity and flow activation energy increase as compared with SFO. The viscosity is influenced by the ozonation time, becoming higher as the ozonation time increases.

Overall, the NMR data confirm that progressive SFO ozonation leads to the formation and accumulation of characteristic products, including 1,2,4-trioxolane derivatives, hydroxy-hydroperoxides, and aldehydes. Simultaneously, the diminishing intensities of linoleic and oleic acid signals demonstrate the steady depletion of unsaturated fatty acids as ozone cleaves the carbon–carbon double bonds through the Criegee's mechanism. These changes collectively highlight the systematic transformation of the oil's molecular structure with increasing ozonation time.

Also, the FTIR spectral changes observed with increasing ozonation time confirm the progressive transformation of SFO through the Criegee's ozonation mechanism, leading to the formation of ozonides, trioxolanes, and subsequent carbonyl-containing products. The reduction of ester carbonyl bands, the growth of characteristic low-frequency signals, and the emergence of C–O– groups collectively demonstrate the breakdown of unsaturated structures and formation of oxidative derivatives. Additionally, the accelerated conversion in the presence of water—evidenced by the disappearance of the 1722 cm^{-1} band—highlights water's key role in promoting ozonide decomposition into aldehydes and carboxylic acids.

The ozonated SFO samples demonstrate strong antioxidant performance across varied mechanisms, exhibiting high metal-chelating and FRAP activity alongside meaningful radical-scavenging and lipid-protection effects. Their ability to act in both acidic and near-neutral environments highlights a broad therapeutic potential.

Declarations:

Funding: This work was supported by a grant of the Ministry of Research, Innovation and Digitization, CNCS/CCCDI - UEFISCDI, project number PN-IV-P8-8.1-PRE-HE-ORG-2023-0048, within PNCDI IV.

Conflicts of interest/competing interests: The authors declare no competing interests.

Acknowledgements: This work was supported by a grant of the Ministry of Research, Innovation and Digitization, CNCS/CCCDI - UEFISCDI, project number PN-IV-P8-8.1-PRE-HE-ORG-2023-0048, within PNCDI IV.

Data Availability: The datasets used and/or analysed during the current study are available from the corresponding author on reasonable request. All data generated or analysed during this study are included in this published article and its supplementary information files.

Authors' contribution statements: Anca-Roxana Petrovici: Conceptualization, Data curation, Formal analysis, Investigation, Methodology, Project administration, Supervision, Visualization, Writing – original draft. **Vasile Paraschiv:** Data curation, Formal analysis, Project administration. **Alina Niculescu:** Data curation, Formal analysis, Investigation, Methodology, Writing – original draft. **Mirela Zaltariov:** Data curation, Formal analysis, Investigation, Methodology, Writing – original draft. **Maria Bercea:** Data curation, Formal

analysis, Investigation, Methodology, Writing – original draft. **Natalia Simionescu:** Data curation, Visualization, Writing – review and editing. **Mariana Pinteala:** Funding acquisition, Project administration, Visualization, Writing – review and editing.

References

1. Romano, R. *et al.* Oxidative stability of high oleic sunflower oil during deep-frying process of purple potato Purple Majesty. *Heliyon* **7**, e06294 (2021).
2. Majcher, M., Fahmi, R., Misiak, A., Grygier, A. & Rudzińska, M. Influence of ozone treatment on sensory quality, aroma active compounds, phytosterols and phytosterol oxidation products in stored rapeseed and flaxseed oils. *Food Chem.* **469**, 142551 (2025).
3. Lužaić, T. *et al.* Investigation of oxidative characteristics, fatty acid composition and bioactive compounds content in cold pressed oils of sunflower grown in Serbia and Argentina. *Heliyon* **9**, e18201 (2023).
4. Jiménez-Hernández, G., Ortega-Gavilán, F., González-Casado, A. & Bagur-González, M. G. Using a portable Raman-SORS spectrometer as an easy way to authenticate high oleic sunflower oil. *Food Control* **177**, 111443 (2025).
5. Guo, S., Ge, Y. & Na Jom, K. A review of phytochemistry, metabolite changes, and medicinal uses of the common sunflower seed and sprouts (Helianthus annuus L.). *Chem. Cent. J.* **11**, 1–10 (2017).
6. Lammari, N., Louaer, O., Meniai, A. H., Fessi, H. & Elaissari, A. Plant oils: From chemical composition to encapsulated form use. *Int. J. Pharm.* **601**, 120538 (2021).
7. Martinez Tellez, G., Ledea Lozano, O. & Díaz Gómez, M. Measurement of Peroxidic Species in Ozonized Sunflower Oil. *Ozone Sci. Eng.* **28**, 181–185 (2006).
8. Roccia, P., Martínez, M. L., Llabot, J. M. & Ribotta, P. D. Influence of spray-drying operating conditions on sunflower oil powder qualities. *Powder Technol.* **254**, 307–313 (2014).
9. Belingheri, C., Giussani, B., Rodriguez-Estrada, M. T., Ferrillo, A. & Vittadini, E. Oxidative stability of high-oleic sunflower oil in a porous starch carrier. *Food Chem.* **166**, 346–351 (2015).
10. Le Tan, H., Ferrentino, G., Morozova, K., Tenuta, M. C. & Scampicchio, M. Supercritical CO2 extraction and fractionation of turmeric polyphenols: Antioxidant capacity and inhibition of lipid oxidation in sunflower oil. *Food Biosci.* **69**, 106906 (2025).
11. Nid Ahmed, M. *et al.* Advances in the Use of Four Synthetic Antioxidants as Food Additives for Enhancing the Oxidative Stability of Refined Sunflower Oil (Helianthus annuus L.). *Anal. 2024, Vol. 5, Pages 273-294* **5**, 273–294 (2024).
12. Ahmed, M. N. *et al.* Saffron (Crocus sativus L.) stigmas as a potential natural additive to improve oxidative stability attributes of sunflower (Helianthus annuus L.) oil stored under different conditions. *Grain Oil Sci. Technol.* **7**, 133–149 (2024).
13. Guerra-Blanco, P., Chairez, I., Poznyak, T. & Brito-Arias, M. Kinetic Analysis of Ozonation Degree Effect on the Physicochemical Properties of Ozonated Vegetable Oils. *Ozone Sci. Eng.* **43**, 546–561 (2021).
14. Sadowska, J. *et al.* Characterization of ozonated vegetable oils by spectroscopic and chromatographic methods. *Chem. Phys. Lipids* **151**, 85–91 (2008).
15. Cho, K. H., Kim, J. E., Bahuguna, A. & Kang, D. J. Ozonated Sunflower Oil Exerted Potent Anti-Inflammatory Activities with Enhanced Wound Healing and Tissue Regeneration Abilities against Acute Toxicity of Carboxymethyllysine in Zebrafish with Improved Blood Lipid Profile. *Antioxidants 2023, Vol. 12, Page 1625* **12**, 1625 (2023).
16. Valacchi, G. *et al.* Ozonated oils as functional dermatological matrices: Effects on the wound healing process using SKH1 mice. *Int. J. Pharm.* **458**, 65–73 (2013).
17. Cho, K. H. *et al.* Ozonated Sunflower Oil Exerted Protective Effect for Embryo and Cell Survival via Potent Reduction Power and Antioxidant Activity in HDL with Strong Antimicrobial Activity. *Antioxidants 2021, Vol. 10, Page 1651* **10**, 1651 (2021).
18. Cho, K. H., Kim, J. E., Bahuguna, A. & Kang, D. J. Long-Term Supplementation of Ozonated

Sunflower Oil Improves Dyslipidemia and Hepatic Inflammation in Hyperlipidemic Zebrafish: Suppression of Oxidative Stress and Inflammation against Carboxymethyllysine Toxicity. *Antioxidants* **12**, 1240 (2023).
19. Petrovici, A. R., Anghel, N., Dinu, M. V. & Spiridon, I. Dextran-Chitosan Composites: Antioxidant and Anti-Inflammatory Properties. *Polym. 2023, Vol. 15, Page 1980* **15**, 1980 (2023).
20. Petrovici, A. R. *et al.* New insights on hemp oil enriched in cannabidiol: Decarboxylation, antioxidant properties and in vitro anticancer effect. *Antioxidants* **10**, 738 (2021).
21. Petreni, A. *et al.* Carbonic Anhydrase inhibitors bearing organotelluride moieties as novel agents for antitumor therapy. *Eur. J. Med. Chem.* **244**, 114811 (2022).
22. Travagli, V., Zanardi, I., Valacchi, G. & Bocci, V. Ozone and Ozonated Oils in Skin Diseases: A Review. *Mediators Inflamm.* **2010**, 610418 (2010).
23. Guerra-Blanco, P., Poznyak, T., Chairez, I. & Brito-Arias, M. Correlation of structural characterization and viscosity measurements with total unsaturation: An effective method for controlling ozonation in the preparation of ozonated grape seed and sunflower oils. *Eur. J. Lipid Sci. Technol.* **117**, 988–998 (2015).
24. Iorio, F. B. R. D., Liberatore, A. M. A., Koh, I. H. J., Otani, C. & Camilo, F. F. Ozonated Mineral Oil: Preparation, Characterization and Evaluation of the Microbicidal Activity. *Ozone Sci. Eng.* **38**, 253–260 (2016).
25. Sega, A. *et al.* Properties of sesame oil by detailed 1H and 13C NMR assignments before and after ozonation and their correlation with iodine value, peroxide value, and viscosity measurements. *Chem. Phys. Lipids* **163**, 148–156 (2010).
26. Chira, N. A. *et al.* Evaluation of the computational methods for determining vegetable oils composition using1H-NMR spectroscopy. *Rev. Chim.* **62**, 42–46 (2011).
27. Chira, N. A., Nicolescu, A., Stan, R. & Rosca, S. Fatty acid composition of vegetable oils determined from 13C-NMR spectra. *Rev. Chim.* **67**, 1257–1263 (2016).
28. Díaz, M., Lezcano, I., Molerio, J. & Hernández, F. Spectroscopic Characterization Of Ozonides With Biological Activity. *Ozone Sci. Eng.* **23**, 35–40 (2001).
29. Díaz, M. F. *et al.* Spectroscopic characterization of ozonated sunflower oil. *Ozone Sci. Eng.* **27**, 247–253 (2005).
30. Rodrigues De Almeida Kogawa, N. *et al.* Synthesis, characterization, thermal behavior, and biological activity of ozonides from vegetable oils. *RSC Adv.* **5**, 65427–65436 (2015).
31. Cirlini, M., Caligiani, A., Palla, G., de Ascentiis, A. & Tortini, P. Stability Studies of Ozonized Sunflower Oil and Enriched Cosmetics with a Dedicated Peroxide Value Determination. *Ozone Sci. Eng.* **34**, 293–299 (2012).
32. Ehsandoost, E., Eskandari, M. H., Keramat, M. & Golmakani, M. T. Antioxidant activity and mechanism of action of phycocyanin in bulk sunflower oil and respective oil-in-water emulsion. *Curr. Res. Food Sci.* **10**, 100981 (2025).
33. Sehim, A. E., Abd Elghaffar, R. Y., Emam, A. M. & El-Desoukey, T. A. Evaluation of the efficacy of ozonated olive oil for controlling the growth of Alternaria alternata and its toxins. *Heliyon* **9**, e17885 (2023).